NCPTT

Rapid Quantification of Ceramic Paste Recipes using Digital Capture and Image Analysis | 2012-14

University of Oklahoma

National Park Service
U.S. Department of the Interior

National Center for Preservation Technology and Training

Narrative Final Report for MT-2210-08-NC-05

Rapid Quantification of Ceramic Paste Recipes using Digital Capture and Image Analysis

University of Oklahoma

Principal Investigator: Patrick Livingood, Associate Professor of Anthropology, University of Oklahoma, 521 Dale Tower, Norman, OK 73072. Email: patrickl@ou.edu. Web site: http://portfolio.ou.edu/users/livi5882/web/

Project Team Consultant: Ann Cordell, Staff Archaeologist, Florida Museum of Natural History, 106 Dickinson Hall, Museum Road & Newell Drive, Gainesville, FL 32611, Email: cordell@flmnh.ufl.edu

Date of Final Report: May 7, 2012

Table of Contents

Executive Summary

This report describes the procedures developed to measure shell temper in the exposed edges of archaeological sherd using digital image analysis methods and provides instructions for how to implement these procedures. It also provides confirmation that using a human-checked version of the algorithms included can produce measurements on the shell temper comparable to what is achieved with traditional microscopic petrography with considerably less time investment. It further applies this method to achieve two results. In the first instance it is deployed to measure inter-sherd variation and in the second it is used to measure inter-household variation at the Moon Site, Arkansas.

Introduction

Archaeologists have long recognized the importance of studying temper in ceramics. Macroscopic analyses of temper are the cornerstones of analyses of ceramic form, function, chronology, style, and technological choice (Rice 1987; Shepard 1976). Analyses at the microscopic level borrow techniques from geology, and identify, count, and measure temper particles and other inclusions. The most common method for accomplishing this is microscopic petrography of thin sections prepared from sherds. This involves the preparation of a thin section and the separate analysis of that thin section by an experienced petrographer who typically uses a cross-polarizing microscope to aid with mineralogical identifications. Microscopic petrography is frequently used as a means of identifying the source of clays based on mineralogical clues, but has also been used to identify and quantify temper inclusions in order to contribute to an understanding of some combination of ceramic form, function, chronology, style, and technological choice (Stoltman 1989, 1991, 2000).

The biggest impediment to more widespread use of ceramic petrographic analysis is the cost involved. Thin section preparation can run $20-30 per sample for a lab. Archaeologists interested in making their own sections must have access to equipment normally only found in geology departments and considerable expertise, however with those the process can be done at about an hour per sample with material costs of a few cents to $2 per sample. Once the thin section is prepared, analyst fees can run $100 per sample or more. The alternative is having access to a petrographic microscope, having considerable training in mineralogy, and the cost of 4-6 hours per sample for a typical point-pointing petrography. With these costs and equipment needs, it is no wonder that ceramic petrography remains underused and, when deployed, it often is restricted to relatively small sample sizes (Livingood and Cordell 2009).

Over the last several years, archaeologists have recognized that digital technologies can assist with various facets of the microscopic analyses of ceramics. Here are some of the applications:

> Digital Microscope – Many researchers have simply found that inexpensive scanners and digital cameras can serve as readily available tools to get images of higher magnification that is easily possible with the human eye (Velde and Druc 1998).
>
> Aid to counting – There are many image analysis programs that facilitate the task of manipulating captured digital images to highlight features of desired interest and/or to count features that have been highlighted by manual or automatic means (Velde and Druc 1998; Reedy 2006; Whitbread 1991).
>
> Aid to identification – Image analysis can easily take multiple views of the same subject under different conditions, such as the use of polarizers or different lighting, and

produce composite, false-color images that aid in the viewing and identification of the object (Livingood 2007).

In my own research, this led to a project in which I analyzed temper of sherds from the Pevey Site in Mississippi in prepared thin sections (Livingood 2010, 2007). The thin sections were scanned using a consumer-grade flatbed scanner and the images were processed using the Image Analysis Toolkit by Reindeer Graphics. The study focused on mapping and measuring three kinds of inclusions (sand, grog, and shell) and used a mix of automated and user-directed methods to map the particle inclusions. Four of these thin sections were also examined by Ann Cordell using traditional microscopic petrography, and the results confirmed that the measurements of grog and shell were acceptably close (Livingood and Cordell 2009).

The big lesson from that work was that the digital approach and the traditional microscopic petrography approach each have questions and applications for which they are better suited. The advantages of the digital approach is that it can be faster and cheaper when it is deployed on a large number of relatively homogenous samples and if it can be partially or wholly automated because the features to be mapped have high visual contrast.

This research is an attempt to test whether under these conditions the digital approach is as effective as it appeared in 2009. In this study, the inclusions we are interested in measuring are shell temper. Shell temper, when it is still present in the archaeological sample, has a high visual contrast from the surrounding ceramic matrix. However, the shell is often leached out of archaeological sherds because of the action of groundwater, and in that case the shell is visible as highly linear voids. Both aspects of shell have high visual contrast. Further, shell and shell-voids are visible in the sherd edge and therefore can be measured without the need to manufacture thin sections. Other researchers have examined extant shell in sherd edges using a digital image analysis approach (Daniels and Lipo 2008; Pereira 2012), but none to my knowledge have evaluated its accuracy against other approaches or attempted to map shell as shell voids. Therefore, this project seeks to discover if there is a rapid, low-cost procedure to measure shell temper in the exposed edges of sherds and to test its accuracy against traditional microscopic petrography. The promise of such a method is that it would permit archaeologists to ask research questions that have, up until now, been unapproachable because of their high costs.

The Ceramic Sample

The measurement comes from sherds from the Moon site (3Po488) in Arkansas (Benn 1992, 1998). The site is a largely excavated palisaded village located in northeastern Arkansas that dates to the Middle Mississippian period (AD 1200-1400). 99.9 percent of the sherds recovered from the excavations were undecorated shell-tempered sherds, which made the sample ideal for this study.

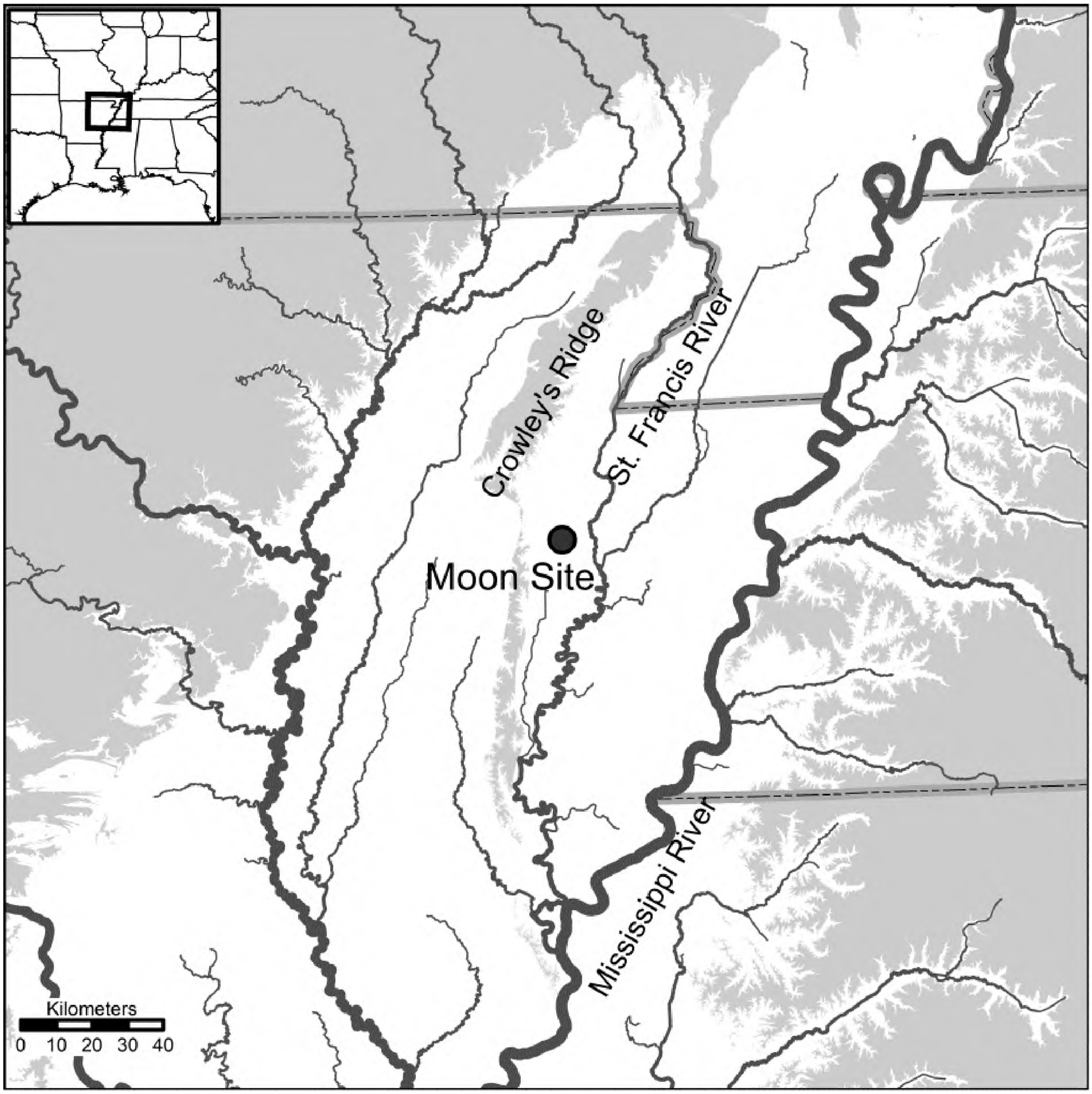

Figure 1. Map showing the location of the Moon site.

Methods

This method works by taking a series of high resolution images of a smoothed and polished sherd edge. These images are then manipulated to create a series of maps. The first map is of the boundaries of the sherd edge. The second map is of extant, visible shell. The third map is of the voids visible after the sherd face has been polished. The map of the voids is created by taking three images of the sherd edge, one with light coming straight on and the other two with light coming from an oblique side angle. By comparing these images it is possible to detect the shadows and to therefore map the voids. The voids with a long aspect ratio are then selected as representing shell.

The general procedure for capturing an image of the sherd edge for analysis are the following:

1. Prepare the sherd edge.
2. Place it on the prepared stage in front of the cameras.
3. Enter data about the sherd in a database.
4. Activate a macro which automatically grabs three images of the sherd edge. In addition, a reference photo of the sherd face was collected.
5. Store the image on a NAS device for later analysis.

What is to follow is a more detailed description of the procedures and equipment used in each step of the process.

Prepare the sherd edge

It is important to create a flattened, smooth, and clean exposed sherd edge for data capture. After much experimentation, we found that the best results came from two stages of sanding and then cleaning with compressed air. Our desire was to find a solution using inexpensive, widely available tools if possible. Sanders are widely available, but we found most disc and belt sanders were inappropriate. If they are rotating at too high of a speed, caused most sherds to crumble during sanding or polishing. The best results were found with a pair of Professional Maker's Mark 10 inch disc sanders (also sold under the name Variable Speed 10 Inch Disc Sander) sold through Micro-Mark. The sanders have adjustable speeds and are capable of very low speeds of 300-400 rpm. These speeds are an order of magnitude less than commercial disc sanders typically found in a hardware store. The sanders used were marked to hobbyists interested in working with balsa wood. These sanders were also made to be hooked up to Shop-Vacs in order to reduce the dust levels.

The first sander was equipped with 360 grit standard sandpaper and was used to make a first pass to flatten an already exposed sherd surface. Depending on the friability of the sherds used, different grit sand paper may be desired, and will require experimentation. 360 grit worked fine for most of our sherds, but some of the sherds with a denser, more compact paste may have benefitted from a coarser paper. The second sander was equipped with 20 micron diamond microfinishing film, which is used to smooth the sherd surface. Special attention needs to paid during this step that the film is not being overused, since that will cause very small grooves to be worn in surface rather than to make a good polish. Additionally, care needs to be taken that the only process that occurs during this step is smoothing, not polishing. Sherds with polished edges reflect too much light during the step involving direct lighting and obscure the sherd surface. Good sample preparation is very important.

After the sherd surface was smoothed it was cleaned using a blast of air from an air compressor equipped with a trigger-activated blow gun attachment. This removed surface dust and removed particles from the surface voids. The equipment used in this process was a Campbell Hausfeld 2 Gallon Direct Drive Quiet Air Compressor, but any small hobbyist air compressor will work. If done in a lab setting you may want to consider issues of noise before selecting a model.

Figure 2. Photograph of circular sander being used to smooth sherd face.

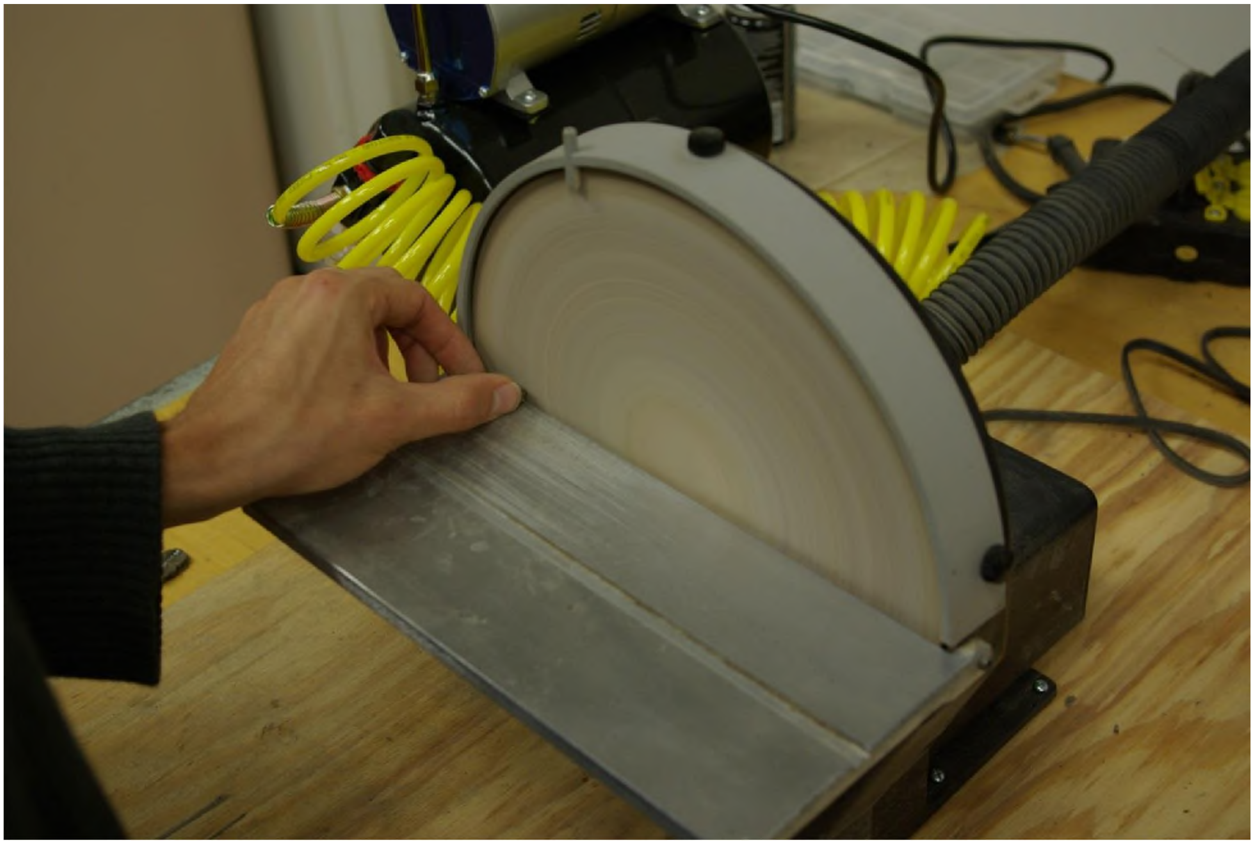

Figure 3. Close up of circular sander.

Figure 4. Top-down view of circular sander.

Figure 5. Photograph of dust being removed from sherd face with air from an air compressor.

Capture of Sherd Image

The image of the sherd edge was generated by a EOS-1Ds Mark III digital camera equipped with a Canon 100mm macro lens. The camera is capable of producing images of 5,632 x 3,750 pixels (21.1 megapixels). At the time of purchase, it was the highest resolution camera model available in a consumer-grade device. Based on early experiments, this was deemed to be sufficient resolution to measure shell inclusions. Based on prior work (Livingood and Cordell

2009), it is especially important to make sure the resolution is a match to the smallest feature of interest. In this case, I suspect that improved accuracy could be achieved by increasing the resolution of image capture, especially for distinguishing fine shell present as voids, but that this current resolution is sufficient. Increasing resolution would be possible today since consider cameras are now made (Spring 2013) with 36 megapixel sensors, but higher resolution also comes with increased storage costs and increased processing time.

There were three images of the sherd edge collected by the EOS-1Ds Mark III camera. The first was illuminated using a Canon MR-14EX ring flash that was attached to the front of the camera. This had the effect of completely illuminating the sherd face and washing out all of the shadows. A second picture was taken while an Alienbees B-800 studio flash illuminated the sherd from a 55 degree angle (55 degrees as measured from the sherd-to-camera axis). This had the effect of illuminating the sherd from the right and casting shadows across the surface of the sherd where voids were present. A third picture was taken while a different Alienbees B-800 studio flash illuminated the surface from the left.

The camera was tethered to a computer via a USB connection and was controlled from the computer using Breeze System's DSLR Remote Pro Multi-Camera software. The three flash units were connected using sync cords. With this technology, the camera issues an electronic pulse via the flash shoe on its top. This signal passes along cords that terminate in 3.5 mm headphone jack-like connectors, which is typically plugged into a flash unit that triggers when the signal arrives. Rather than have the camera trigger a single flash every time, the system for this project was made controllable and flexable. The outgoing flash sync cord from the camera as well as the input sync cord for the three flashes were all plugged into a NCD R810PRO electronic relay control. Electronic relay controls allow the computer to issue commands to physically rearrange the circuit to connect certain devices while leaving other devices unconnected. Prior to the first image being taken, the computer issued a command to the relay to connect the circuit between the camera camera sync output and the ring flash input. Therefore, when the camera was ordered to take a photograph and it sent the pulse to the flash sync, only the ring flash unit actived. Before the second image, a command was sent to the relay to only connect the single studio flash unit and the camera output and so on. As a result, the computer could rapidly send commands to gather the three images using the three required flash configurations. The computer code for interacting with the relay and the camera will be posted to the PI's web site.

Some of the additional equipment needed to connect this apparatus include a 'USB to RS-232 Serial Adapter Compatible with PC/MAC and NCD Devices' to connect the NCD R810PRO relay to the USB port of the computer. Also a 'Quantum Instruments Battery Pack - Turbo AC Universal Battery (100 - 240 VAC)' was used to power the Canon MR-14EX ring flash, and a

‘Kaiser PC to Hot Shoe Adapter’ and a ‘General Brand Sync Extension Cord - PC Male to PC Female ‘ was needed to connect the flash to a sync cord.

In addition to the images captured of the sherd edge, a single image was captured of the sherd face for reference and study. This image was captured using a Canon EOD 40D Digital SLR camera using a ‘Canon ACK-E2 AC Adapter Kit’ to replace battery power. The camera was attached to another Alienbees B-800 studio flash.

The entire apparatus was physically arranged in the following way. A wooden table was used to support the sherd for photography (a plywood bench found at surplus). The table was covered in black felt, measurement scales, and color reference cards. A piece of plywood was attached to a spring-motion hinge on the table edge. The hinge selected is typically used in cabinet furniture and it springs readily to a fully open or a fully closed position. Further, when the plywood guide was raised, it stood up vertically, was held in position by the hinge, and created a barrier that one could place the sherd edge against. This gave the worker doing the data collection a way to know where the camera field of vision is located and to ensure that the sherd edge was consistently placed at the same distance from the camera. The wooden bar could then be flipped down to allow photography of the sherd edge.

The EOS-1Ds Mark III camera, ring flash, and two B-800 studio flash were placed on a scaffold facing the wooden table. The scaffold was a heavy duty shelving unit with plywood shelves; this permitted flexibility in arranging the height of the shelves and also attachment points for other pieces of equipment. The EOS-1Ds Mark III camera was mounted on a ‘Adorama Macro Focusing Rail Set’ which permitted fine movements and a ‘Jobu Design 2 Axis Flash Hot Shoe Bubble Level’ permitted us to easily check for level. The Two B-800 flash units were mounted to the scaffold at the same plane as the camera and at the 55 degrees from the sherd face. The flash units were still relatively close to the sample and were equipped with ‘Alienbees HG20 20 degree grid’ inserts to help reduce the light from incidental angles.

On top of the wooden table was mounted a camera reproduction stand holder which held the Canon EOD 40D Digital SLR over the sample. The flash it was attached to was attached to the scaffold at a similar horizontal level.

The table and the scaffold were both mounted to a plywood base to provent movement and vibration during photography, and the entire apparatus was then shroud in back material (a pair of black fabric shower curtains suspended from plastic shower rods) that could be pulled back with ease to permit access to the sample and equipment. This permitted us to reduce incidental light during photography.

Figure 6. Photograph of image capture apparatus.

Figure 7. Closeup of image capture apparatus.

Figure 8. Close up of stage for sherd. This shows the placement board in the up position. It could be flipped down when it is time for image capture.

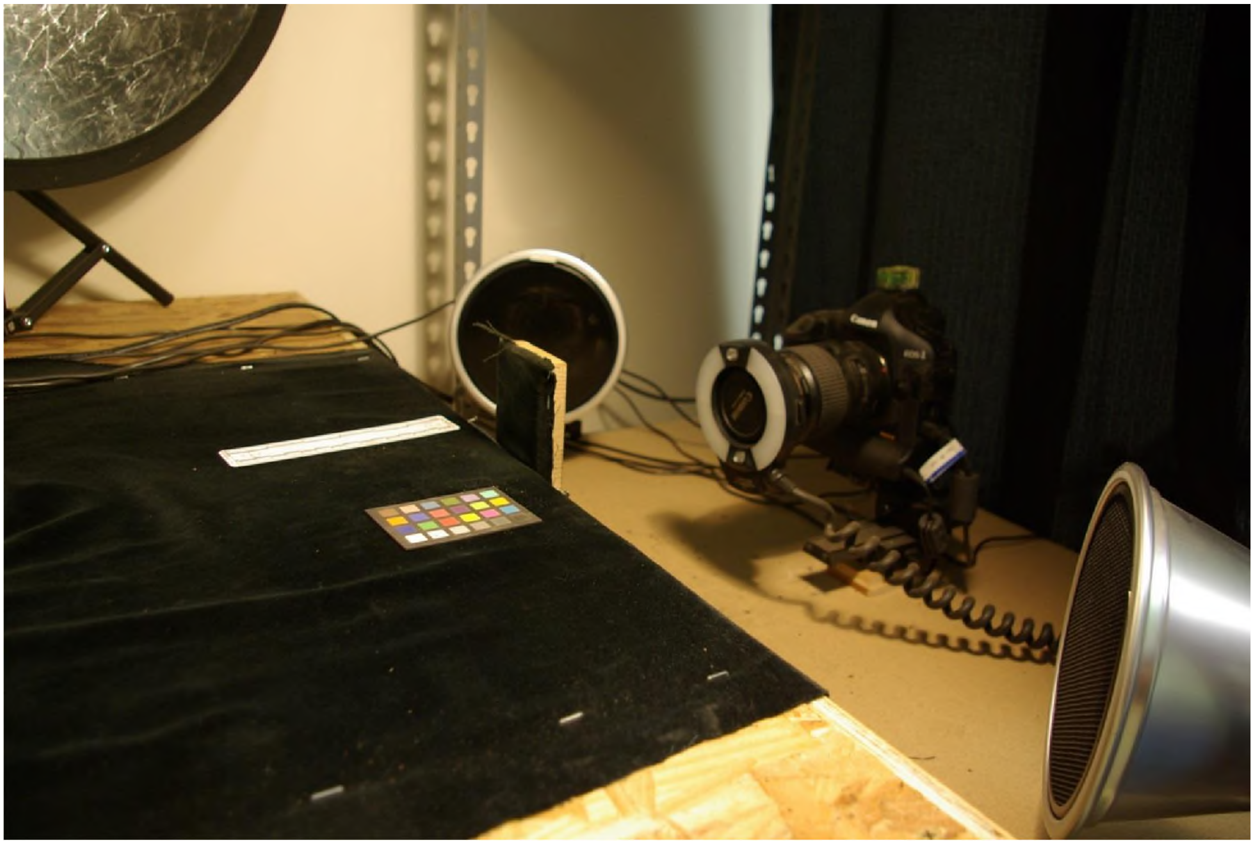

Figure 9. Another close up of the image capture stage, with Mark III camera visible.

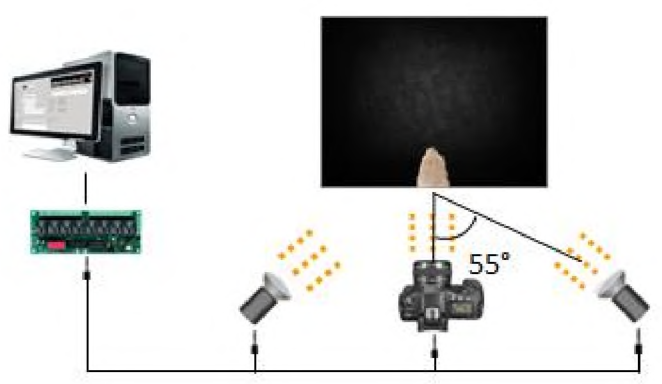

Figure 10. Schematic overhead visualization of the arrangement of the Mark III camera and ring flash units.

Figure 11. Example capture image of sherd face using ring flash.

Figure 12. Example capture image of sherd face using flash from the right.

Figure 13. Example capture image of sherd face using flash from the left.

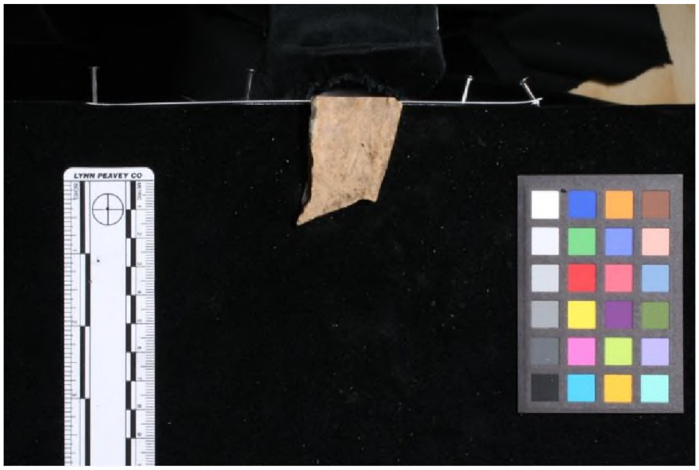

Figure 14. Example image of sherd face.

Computer Control of Capture Process

The process of image capture was designed to be as rapid as possible and to be a process that could be done by relatively inexperienced undergraduate students. Their primary workflow at the computer was the following once a sample is placed in the stage for image capture:

1. At the beginning of the day, and at regular intervals, access the camera controls using Breeze System's DSLR Remote Pro Multi-Camera software and check and adjust focus as necessary.
2. Open (or have open) the Microsoft Access database used to store data about the samples. A single form is used by the operator. Enter in the provenience data for the sample and record any relevant macroscopically-available information.
3. Press a single button which triggers a macro that captures, displays, and stores all of the images. This step took about 7 seconds to run.

The entire process of sherd preparation, data entry, and image capture averaged about 3-4 minutes per sherd, although there was fairly significant variation between workers and over time. The code that was used in Access to trigger the image capture will be posted online at the PI's website.

The macro saved versions of the images to a NAS Server where all of the data was placed. Images from the Mark III camera were saved in RAW format and the sherd face image from the 40D camera was saved as a JPEG. All four of the images together average about 64 MB worth of data. Once analyzed, the completed Photoshop files containing both the original sherd edge images, completed maps, and interim processing images average 238 MB. This means that storage costs for each sample average 302 MB, not including backups.

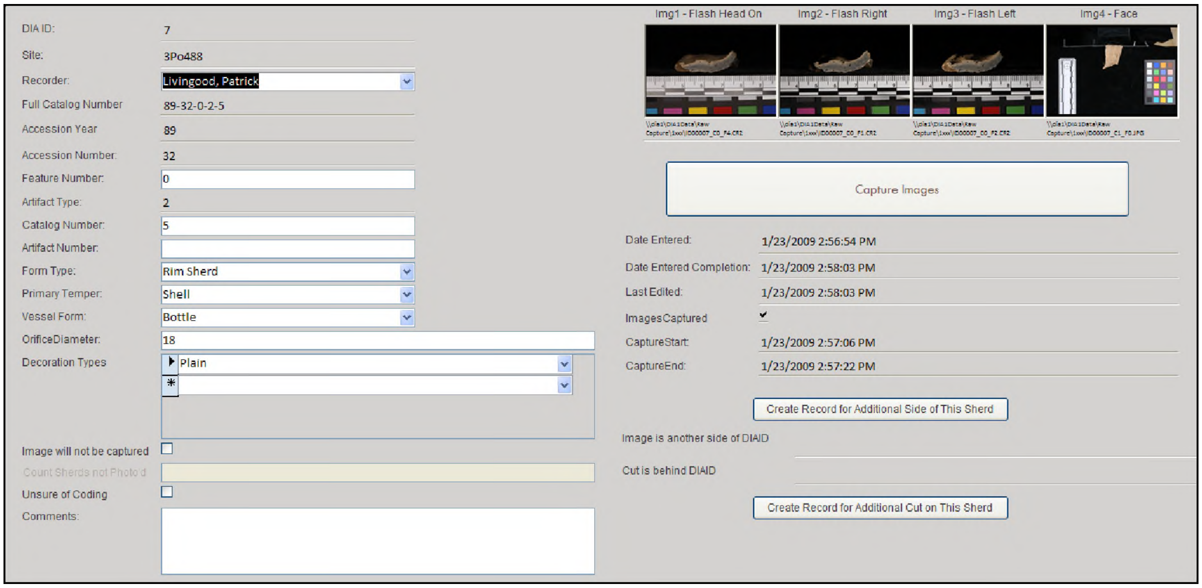

Figure 15. Microsoft Access form used for data entry and image capture.

Digital Processing of Results

The current best method for processing the digital images to measure the shell temper involves some instances of user intervention as documented below. The process is still rapid, but the algorithm to make this more robust and fully automated has not yet been developed. Attempts to make this algorithm more automated and involve less user intervention are ongoing, and updates to this algorithm will be placed at the PI's web site.

The software used for this process is Fovea Pro by Reindeer Graphics, which runs as a series of plugins for Adobe Photoshop. These steps can be automated using Photoshop's built in macro recording tools or alternatively scripted using Photoshop's Scripting language.

The principals of digital image analysis are summarized in these steps: first process the image to enhance the feature class of interest, then select the features of interest using some form of thresholding based on classifiable visual characteristics to produce a Boolean image in which pixels are either black to indicate that they are part of a feature or white to indicate that they are not, and finally to use the Boolean image as an input to a function that counts and measures all of the features (Russ 1999).

The following chart provides an outline of the procedures followed to perform the analysis. User intervention came in two forms during this process. First, for each of the major maps, there were several different recipes developed. In the current incarnation of the workflow, an initial run was made to produce several different initial results, and the best one was selected by hand. One of the most crucial steps of creating the maps is the threshold step. In this step, all pixels greater than a certain value related to color, intensity, or darkness are classified as on and all others are classified as off to create a Boolean image. There are several automatic algorithms which pick a threshold value based on characteristics of the histogram of values. These frequently work quite well, but in some cases they are clearly too conservative or too aggressive and a manual adjustment of the threshold value was called for.

In the directions, I provide a general description of the process and I also provide the steps using Photoshop and Fovea Pro commands. All of these commands are found widely in other image processing suites and this analysis is not restricted to just this software.

Table 1. Description of the digital image analysis algorithm.

General Description	Fovea Pro Commands	Example Images
Images are loaded in as separate layers. In this process, images are labeled F1 and F2 for the obliquely lit samples and F4 for the sample illuminated by the ring flash.		 F1 Image 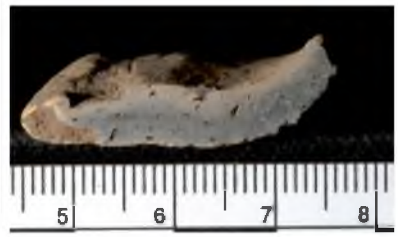 F2 Image  F4 Image
Measurement Calibration. Based on the scale the measurement of pixels to units is calibrated.	Measure Global | Calibrate Magnification (this is recalled between runs and does not need to be updated if the scale remains constant between images).	

General Description	Fovea Pro Commands	Example Images
Remove Scale. The scale is eliminated with the application of a standard mask or the image is cropped to remove the scale.		 F1 Image  F2 Image  F4 Image
Make a Shadows layer that at every pixel location uses the darkest pixel value of the three images.	a. Duplicate F4 - Call 'F4 - Shadows' b. Make F1 2nd Image c. Apply against Shadows – Select Darkest (Math – Keep Darker Value) d. Make F2 2nd Image e. Apply Against Shadows – Select Darkest	 F4 – Shadows

General Description	Fovea Pro Commands	Example Images
Make a Sherd Face Mask. This is a Boolean image that represents the outline of the sherd face. There were several different recipes developed for this that were run automatically. The algorithm presented on the right was one of the most commonly used. The next most commonly used was simply using 'Sherd Face Mask 2' The Sherd Face Mask 1 recipe is simply a threshold of the Shadows layer. Mask 2 is made by creating an image that is created by multiplying the pixels of F4 and the Shadows image and then thresholding. Mask 3 (not described at the right) uses the magic wand tool in Photoshop to select a contiguous area including the background and then to invert the selection and clean. No matter which Mask was selected, it was important to clean the resulting mask of stray signals. This was successfully done in almost all cases by Rejecting all features smaller than 3000 pixels, by filling all of the holes in the feature, by shrinking the area by 2 pixels using the EDM Open operator, re-rejecting all features smaller than 3000 pixels and only retaining features of breadth 3+ mm.	1. Make Sherd Face Mask 1 a. Duplicate Shadows to 'Sherd Face Mask 1' b. Bilevel Threshold 2. Make Sherd Face Mask 2 a. Duplicate F4 to 'Sherd Face Mask 2' b. Make F4 Shadows 2nd Image c. Apply Against Sherd Face Mask 2 – Math | Multiply d. Bilevel Threshold 3. Make composite Sherd Face Mask from 1 and 2 a. Duplicate Sherd Face Mask 1 – Call 'Sherd Face Mask' b. Make 'Sherd Face Mask 2' 2nd Image c. Boolean Operator OR d. Invert 4. Clean Sherd Face Mask a. Reject Features – 3000 b. Fill Holes c. EDM Morphology... Open 2 d. Reject Features 3000 e. Select Features... minimum breadth 3+ mm	 Sherd Face Mask 1  Sherd Face Mask 2  Sherd Face Mask

General Description	Fovea Pro Commands	Example Images
Make a Sherd Face Outline. This is a Boolean image that overlaps slightly inside and out of the sherd edge and is used in later operations. The routine uses the Sherd Face Mask from the previous operation and begins with a Find Edge process. Then the edge is dilated by 2 pixels	a. Duplicate Sherd Face Mask to Sherd Face Outline b. Find Edge, Sobol Method c. EDM Morphology, Dilate 2	
Make Voids Layer This is the most common recipe used for identifying voids. In some cases a manual override is needed in the thresholding step. First a temporary layer is created called Voids 1 that is made by subtracting F4 from the F4 Shadows layer and then thresholded. This will tend to also pick noise around the sherd edge. In order to clean that, all of the Voids 1 features touching the edge are rejected.	1. Make Voids 1 Layer a. Duplicate F4 Shadows to 'Voids 1' b. Make F4 2nd Image c. Apply Against Voids 1 – Math | Subtract d. Make Sherd Face Mask 2nd Image e. Mask by 2nd f. Threshold 2. Reject Edge Voids a. Duplicate Voids 1 to Edge Voids b. Set Sherd Face Outline as 2nd Image c. Math | Select Features by 2nd d. Duplicate Voids 1 to Voids e. Set Edge Voids as 2nd Image f. Math | AND Not 2nd g. Filter | Reject Features …. 20	 Voids 1 Layer  Edge Voids Layer  Voids layer
Make Shell Voids Layer All voids with aspect ratio greater than or equal to 2 are selected as shell voids.	a. Duplicate Voids to Shell Voids b. Morphology | Fill Holes c. Select Features: Aspect Ration >= 2	 Shell Voids

General Description	Fovea Pro Commands	Example Images
Make Extant Voids Layer Using the F4 image, all areas of high intensity are selected as potential extant shell. In practice, only images with high intensity color channel values in the F4 layer are checked for extant shell inclusions.	a. Duplicate F4 to Extant Shell Shell b. Make Sherd Face Mask 2nd Image c. Mask by 2^{nd} d. Threshold Intensity, minimum value 200	NA in this sample

Following the completion of these procedures, the boolean images are counted and measured. Under Fovea Pro this command is labeled 'Measure All Features…'

Supervised vs Unsupervised Measurement

The ideal, and long time goal of this researcher, is to develop a single robust set of algorithms for producing the measurements unsupervised. In this study several different impediments were found that frustrated or complicated this goal.

1. Sample preparation or image capture was not ideal in every case. This included insufficient polishing that left striations on the sherd edge that cast shadows. It also occasionally included over-enthusiastic polishing of a dense sherd surface that lead to the development of a sheen. In other cases it involves the placement of the sherd slightly forward or back of the stage leading to a slightly out of focus image. Or it involves a sample that was bumped and was photographed slightly tilted. Unfortunately, it is challenging to detect all of these problems at the time of data recovery, even by attentive workers. Some of these deficiencies can be tested for, or even corrected, using digital solutions after the fact. However, each of these complicates the algorithm considerably.
2. Paste color can vary tremendously from light to dark between sherds. Algorithms need to be adaptable to both and that can be challenging.
3. Paste color can vary across the sherd's cross-section. The boundary between especially light and dark bands can simulate shadows or boundaries to some algorithms.
4. Sherd edge margins are sometimes indistinct. This is analogous to the problem of edge crumble or destruction that can happen with thin section preparation. In this case, it can lead to ambiguity about the size of the sample and therefore the percentages to which sample size serves as a denominator. It can also lead to added difficulty in mapping inclusions near the edges.

These issues are not insurmountable. However, at the moment a supervised algorithm consistently outperformed any single unsupervised algorithm for the measurement of shell and that is what is used in the following tests.

Comparison of Costs

The analysis of petrographic thin sections using microscopic petrography costs about $120 per sample if one were paying to have a thin section made and a petrographer analyze the sample. In contrast, the digital approach has high upfront costs but low per sample costs. This project involved the upfront purchase of approximately $22,000 in cameras, computers, and equipment. That value would be closer to $17,000 today because of the drop in price in comparable cameras. In addition, the per sample expendables, which include hard drive storage space, sanding paper, lapping paper cost 5-8 cents per sample. That price would be 4-7 cents per sample now because of the reduced hard drive costs. In addition there are 3-4 minutes of time or labor costs to prepare each sherd, enter data in a database, and photograph. Finally, in the current workflow there was an average of approximately 5 minutes of checking, and potentially modifying, the digital image maps for each sherd. This varied tremendously between sherds. In some cases the time was less than one minute to confirm the accurate mapping by the algorithm in some rare instances it took 10-15 minutes for the development of maps for particularly idiosyncratic samples or samples with flawed captures as discussed previously.

In summary, this digital approach has significantly lower cost, especially when the upfront costs can be leveraged across large sample sizes, and when the samples are homogenous and amendable to more highly automated processing.

Results and Discussion

Using these procedures, there were three types of analyses that were conducted for this report. The first involved comparing the results of the digital image analysis method to the results obtained by traditional ceramic petrography. The second involved the reanalysis of several different repeated cuts of individual sherds to measure variation within a sherd. The final involved the assessment of variation between the ceramics of distinct households to evaluate the nature of interhousehold variation.

Test of the Accuracy of the Method

Samples were chosen at random from the Moon site ceramic assemblage and thin sections were made from these samples and analyzed by Ann Cordell, a ceramic petrographer. Her complete results will be posted in an appendix to the posted to the PI's web site. As explored previously (Livingood and Cordell 2009), the petrographer' s analysis of the ceramics contains information on much more than just shell temper. It includes identifications of mineralogical inclusions, information on sherd voids and compactness, and information about the paste. For many applications this is critical data and the type of analysis offered in this report is too narrow. However, this analysis is concerned with measuring temper, and it was important to evaluate how accurate it is when compared with traditional methods. The following analysis and writeup was made in conjunction with Ann Cordell.

There are numerous reasons to expect that the digital image analysis of a sherd edge and the petrographic analysis of a thin section should not yield identical measurements of shell abundance. First and foremost, while each method considered the same sherd, it was impossible for these methods to examine precisely the same plane through the sherd. Sherd edges were photographed for the digital analysis and then pieces were cut for thin sectioning, such that a precise correspondence between sherd edge and thin section is not possible. Second, most of the measurements are based on shell voids, which are open to some level of subjective interpretation (see discussion below).

The basis for comparison of petrographic and digital percentages also differs. Petrographic percentages represent reliable estimates of particle abundances. In this study, percentage of shell temper was calculated using the total number of point counts of shell divided by the total number of point counts (excluding non-shell voids). In contrast, the digital shell percentage is calculated as shell divided by the area mapped as the polished sherd edge.

Table 2 shows the comparison of shell abundance measurements of the two methods and Figure 16 shows this comparison in graphical form. In general, the methods agree fairly well, accounting for the possible sources of error. Just to put these values in perspective, the petrographic analysis of these samples averaged measuring 255 point counts per sample. Thus, if a single measurement of shell was added or subtracted from any sample, on average this would change the shell abundance by 0.39 percent. Thus a difference of 0.3 percent shell measured in Sample 1 is the magnitude of a single point count difference, and is thus fairly small.

For the most part, there appears to be few systematic differences in the measurement, though as a group, the digital method is ever so slightly likely to undercount shell. The largest differences by magnitude are to be found in Samples 6, 23, and 25, all of which have differences between 3 and 4 percent. By magnitude of the total shell present, the biggest differences are in Samples 6, 10, 16, 18, and 25, wherein the difference between the two values as a percentage of the petrographic measurement exceeds 15 percent.

In developing the digital image analysis algorithm, we anticipated several possible problems with systematic error that will be evaluated here. One of our initial concerns for this project was that the smallest inclusions may be systematically undercounted because of resolution and focus issues. This was an issue for the smallest birefringent particles in the initial study that compared digital and petrographic point-counting approaches to the study of thin sections (Livingood and Cordell 2009). However, in this study there does not appear to be a systematic undercount of shell based on particle size. If one calculates the correlation between discrepancy (difference between the shell percentages) and the petrographically-measured number of shell in the very fine or fine size category, there is a very low positive correlation ($r=0.10$).

Another concern was that there could be systematic error related to the largest shell inclusions. In this case the correlation between discrepancy (difference between the shell percentages) and the petrographic counts of very coarse or larger shell is still small ($r=0.21$), but indicates that larger particles could be causing more error. This could be explained by a few factors. First, one would expect more overall variance in the sources of error for sherds with large shell because of quantization issues. A void has to be either categorized as a shell void or as a void with a different origin and a single subjective decision (see below) can have a significant outcome on the results if the void is large. A sherd with lots of large voids creates more opportunities for higher divergence with more of these judgments. Second, large very closely spaced shell particles are more likely to be accidentally measured as one mega-particle using the digital image analysis method. This has been observed in a few instances where the gap between the shell voids is very small and is effectively ignored by the algorithm, thus artificially, if slightly, inflating the measurement of shell percentage.

A final concern was that voids in the matrix might be systematically miscategorized as shell or visa versa. The correlation between the percentage of voids in the petrographic samples and the discrepancy between the two methods is a moderate $r=0.50$. This suggests that 25 percent of the differences between the digital and petrographic measurements can be accounted for by the void frequency in the sample as measured by the petrographic method. This is the largest potential source of identifiable error. While this may indicate a systematic problem, we are inclined to view this as a product of the somewhat subjective nature of categorizing voids as being the product of leached shell or of some other process. In support, the petrographic results showed that there is a smaller correlation between void and shell frequencies ($r=0.41$). While this may indicate that sherds with more shell also were more porous, it more likely points to the subjective nature of categorizing voids. The differences between the digital and petrographic analyses can therefore be seen as error that is inherent to the process.

In summary, this provides validation that the method described in this report can measure shell in a way systematically comparable to microscopic petrography, which is the traditional and proven method of making such measurements.

Table 2. Percent difference between digital image analysis and petrographic data for shell abundance (percentage of the difference value as a percentage of the petrographic measurement)

Sample Number	Petrographic Shell Percent	Digital Shell Percent	Difference	Percentage Difference
1	3.72	3.42	0.3	8.1%
2	14.98	13.96	1.02	6.8%
3	10.81	10.67	0.14	1.3%
4	16.06	16.51	-0.45	-2.8%
5	14.44	16.32	-1.88	-13%
6	18.8	22.03	-3.23	-17.2%
7	11.47	11.28	0.19	1.7%
8	11.59	10.28	1.31	11.3%
9	5.86	5.15	0.71	12.1%
10	11.9	13.97	-2.07	-17.4%
11	13.88	13.8	0.08	0.6%
12	8.53	7.38	1.15	13.5%
13	14.74	14.24	0.5	3.4%
14	9.83	10.49	-0.66	-6.7%
15	7.54	7.74	-0.2	-2.7%
16	13.06	11.03	2.03	15.5%
17	16.67	18.23	-1.56	-9.4%
18	12.14	10.07	2.07	17.1%
19	10.66	11.38	-0.72	-6.8%
20	11.2	12.27	-1.07	-9.6%
21	10.76	9.59	1.17	10.9%
22	8.03	7.07	0.96	12%
23	25.47	28.97	-3.5	-13.7%
24	21.81	22.65	-0.84	-3.9%
25	14.62	18.07	-3.45	-23.6%

* negative percent indicates digital result was less than the point count result

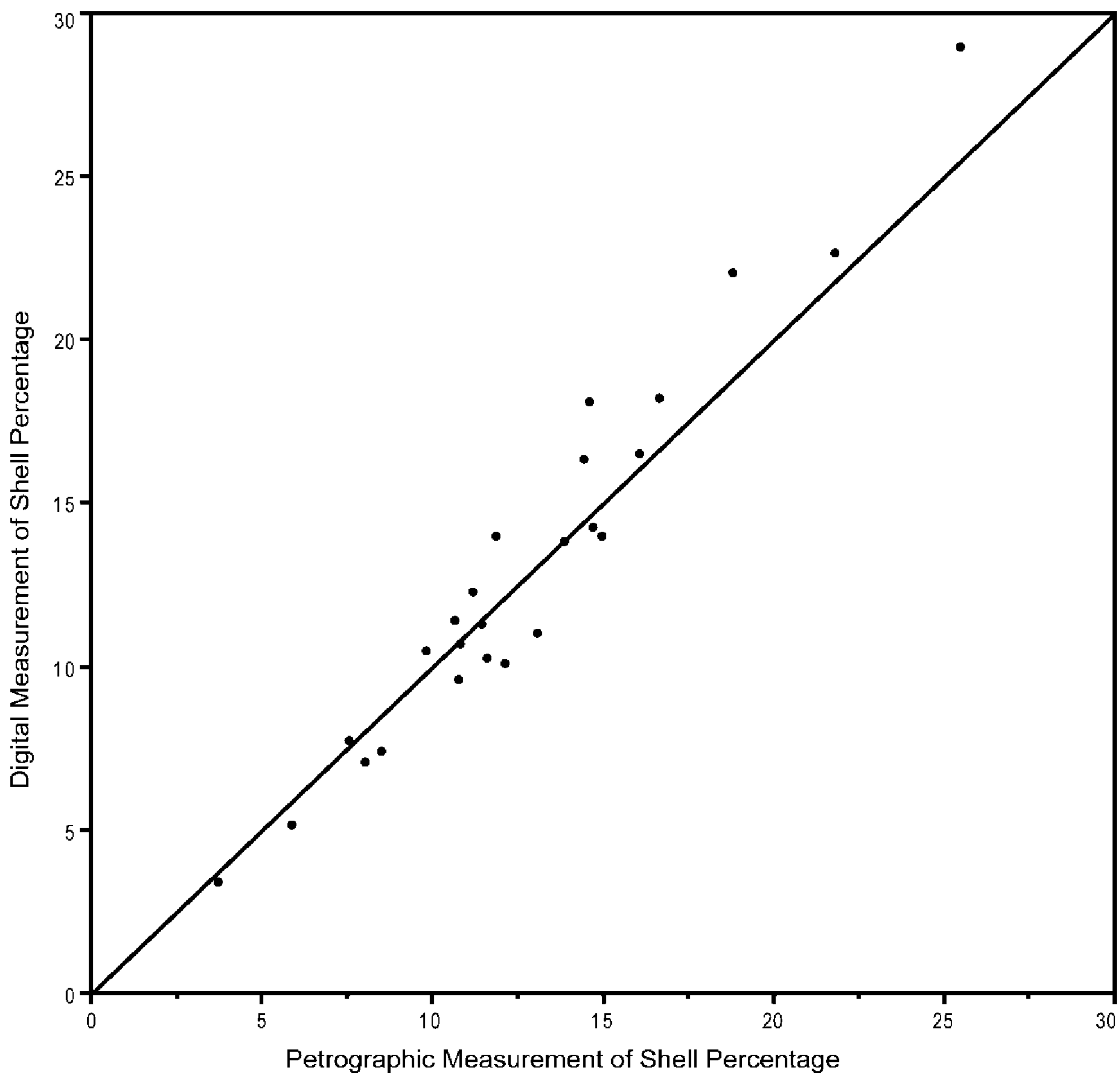

Figure 16. Plot of comparison of shell percent abundance between digital and traditional petrographic measurements.

Evaluation of Inter-sherd variation

As noted above, petrographic analyses involves the observation of a two dimensional surface, sometimes called a section, that is a single slice through a three dimensional matrix. Inclusions in the matrix are necessarily unevenly distributed, which means that a single slice of a specimen can be thought of as a single sample measurement which is assumed to be representative of the whole. Petrographers have long understood this. If one produces multiple thin sections from the same specimen and measures them, one will get slightly different results. Because of the cost involved, traditional petrographers are rarely able to evaluate this directly. Stoltman (1989) observed on a few specimens that this variation is usually less than three percent. More generally, the field of stereology has developed approaches for dealing with the problems inherent with the spatial interpretation of sections.

The digital approach, by lowering the costs of measurement, can provide petrographers with baseline data on observed variation. This research looked at the variation in seven samples, which is far larger than any other study this author is aware of. In each case, an edge was photographed and then approximately 1 mm of material was removed using the sander and the process was repeated.

The only quantity being assessed in this test is the percentage of surface area of the sample that is measured as shell inclusion. Observed variation between sections is a reflection of differences in the true abundance of shell and also of measurement error. The results in Figure 16 and Table 3 show that in some cases, particularly samples 1 and 2, the measurement values agree strongly which is confirmation that the problems of measurement error are small in some cases. In other cases, especially for samples 3 and 8, there is a spread of as much as 6.2 percentage points between the minimum and maximum values.

Further evaluating the results, if we assume the average of the five sections for each sherd is a proxy for the true value of shell, and compare the difference between each section value of shell abundance and the average of the values for the sample, we get the histogram in Figure 17. Here 23 (56%) of the 40 measurements are within 1%, 12 (30%) of the 40 measurements are between 1% and 2% different, 4 (10%) are between 2% and 3%, and there is a single outlier in which the section measurement differs from the average sample measurement by 3.4%.

An examination of the samples with significant spread between values offers some explanation. In the cases of samples 7 and 8 there is a clear appearance of one or two large shell inclusions in one or two of the sections that is absent in the others. Those differences clearly reflect variation in the shell abundance throughout the matrix. In the case of Sample 3, the sample sherd is rather small, which means that small variations in the observed size of the sherd lead to large variations in the percentages. Further, the sherd is relatively friable which leads to indistinct margins for the shell voids. I attribute the majority of the variation in the section measurements of this sample to measurement-related error.

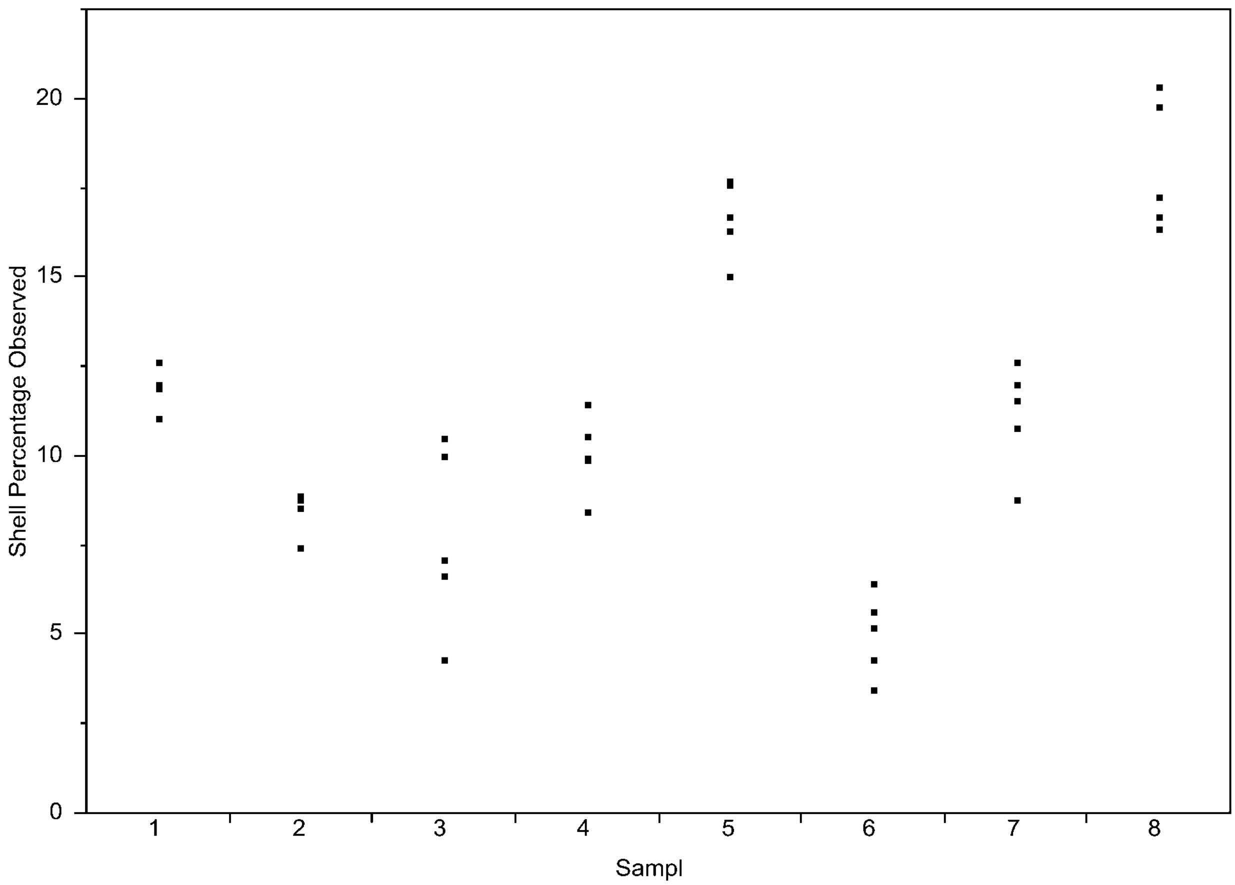

Figure 16. Dot plot of the shell temper measurement as calculated as a percentage of the area by sample. Each dot reflects the measurements made for a single slice and the spread of the dots indicates variation.

Table 3. Results of intersherd variation showing average and minimum and maximum measurements for each sample.

Sample	Average Shell Percentage Measurement	Minimum Shell Percentage Measurement	Maximum Shell Percentage Measurement	Difference between Maximum and Minimum
1	[illegible]	[illegible]	[illegible]	1.6
2	8.5	7.4	8.9	1.4
3	7.7	4.3	10.5	6.2
4	10.1	8.4	11.5	3.0
5	16.7	15.0	17.7	2.7
6	5.0	3.5	6.4	2.9
7	11.1	8.8	12.6	3.9
8	18.1	16.4	20.3	4.0

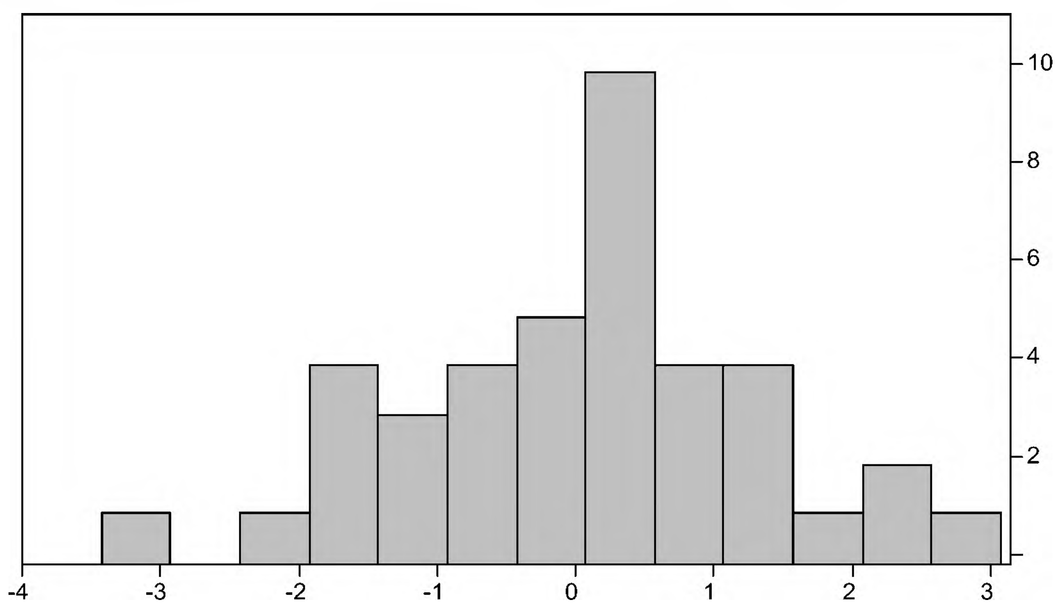

Figure 17. Histogram of the variation in the difference between each section measurement and the average of all measurements for the sample.

Evaluation of Household Variation

A function of the low-cost and high-speed of the digital approach to measuring shell means that it is now feasible to look much more closely at intra-site variation in tempering practices. The study below represents a first step in exploring one aspect of that variation, namely whether it is possible to document inter-household variation in temper practice.

The Moon site, from which the test samples were obtained, is a fairly large palisaded village that was largely excavated. The excavated portion of the site measures about .6 hectares. The investigators documented approximately thirty discrete households clustered around a plaza. Unfortunately, the plowzone cut away the floor surface of most of the structures, so most of the sherds from secure contexts come from features and only a small percentage of the features can be securely associated with a structure (Benn 1992, 1998).

If the researcher is interested in knowing whether there are detectable differences in household temper practice related to learned technological choice, there are some confounding variables that must be considered

1. Although the Moon site was occupied for a relatively short period of time between AD 1200 and 1400, this was long enough that several houses were rebuilt. At the nearby Priestly site, the investigator documented increases in shell-temper abundance that appeared to be temporally related (Benn 1992, 108). We must be aware that variation through time is possible, although there is no way to control for it in this particular study.
2. Potters adjust temper, in part, to account for variations in clay. It may be possible that variations in tempering practice relate to potters obtaining clays from different sources rather than to distinct preferences between the potters of different households. There is no way to control for this factor at the moment.
3. Potters certainly adjust paste recipes to match the intended form of the vessel. Benn's (1992) analysis of rim sherds from Moon suggest that bottles have a higher sand content than other vessel forms, for example. It is possible to control for this using analyses of rim sherds, but this particular analysis uses only body sherds.
4. The recovery of a sherd from a household is not evidence that sherd was manufactured in that household. Benn (1992, 112) considered this issue explicitly in his consideration of the question. For this effort, the households selected for analysis all had mats of gray silty clay that Benn thought were indicative of pottery production. Although we cannot be certain that any individual sherd was made at the household, we can have some confidence that pottery production at least took place at the structures in question. Further, only contexts that the original excavator thought were clearly associated with the household were considered for analysis.

5. This study only measures shell temper. To the extent that paste recipes would have involved other inclusions, those will be missed in this study. In the case of the Moon site, shell tempering is far and away the predominate tempering agent. Sherds also contain sand, but Ann Cordell, citing petrographic data, and David Benn (1992, 108), citing macroscopic evidence, argue that sand is most likely a natural inclusion in the Moon site sherds. This does not mean clay sources were not selected based on their sand content, but it does mean that potters were likely not intentionally adding sand to the paste.

With those caveats in mind, this effort examined thirty randomly selected sherds from each of three different households at the site summarized in Table 4 and a map showing the location of the structures is at Figure 18. The households were chosen because they were all suggested by Benn of being likely loci for ceramic production. Further, they are distributed in different parts of the site.

Based on studies of fresh-water mussel shells as a tempering agent, we know that the shell had to be cooked and then ground. Potters would have had choices about how finely and consistently they would grind the shell and whether they would include all of the shell from their effort, take a pinch from a pile which would select a more homogenous size range, or use some other method that could increase or decrease variability in shell particle size. Benn (1992,93) noted that some of the sherds from Moon had a soapy feel which he attributed to microscopic shell particles in the paste likely caused when the potter emptied all of the residue from grinding shell into the clay.

One of the advantages and the challenges of this digital approach is that it returns a tremendous amount of data about each sherd. Each shell inclusion is mapped, counted, and measured. This provides lots of potential information about potter shell tempering practice. Not only is there data bout the selection of quantity of temper, but there are also data bout temper size and consistency.

For this analysis, the complexity was reduced in order to facilitate analysis. First, shell was classified into four size grades and counted. Then the values were normalized within each size field. Table 5 shows the data from the first five samples in the study, and the rest will be posted to the PI's web site.

From these data, several techniques can be used to help partition the data to look for potential paste recipes. The most direct is cluster analysis. A hierarchical Ward's method cluster analysis was run and the scree plot was examined for elbows to determine if there is an ideal clustering solution. The scree plot elbow is located at six clusters. K-Means clustering was then used to partition the sherds into six clusters. The mean value of the six clusters based on counts of shell within each size category are listed in Table 6 along with descriptions of each temper mode.

The next question is whether or not there is observable household variation in the frequency of sherds with each household (Table 7). The results clearly indicate significant household variation. Structure 51 contains mostly sherds from Cluster 3 (lots of all size shell) and Cluster 5 (very few shell) sherds. Structure 463 has mostly Cluster 1 (lots of small shell), Cluster 3 (lots of all shell size), and Cluster 5 (very few shell). Structure 1104 is fairly evenly represented by all shell types. The chi-square test for this table is significant at $p=.0078$ ($\chi^2= 23.9$), but it is suspect because of the large number of zero and low values in the table. Qualitatively, certain patterns are striking. Cluster 4 sherds are only found at Structure 4. Cluster 1 sherds are absent from Structure 51. The other clusters are more equitably distributed across households.

In summary, this test indicates that there are possible modes in tempering practice and that there are certainly variations between the three households when it comes to abundance of each temper mode. This suggests that such research may be a fruitful avenue for future research.

Table 4. Summary of the Moon site structures analyzed.

Structure	Associated Features	Notes
51	51	There were two different structures built at this locus over time. Located in the northeast corner of the site. (Benn 1992, 443)
463	463, 497, 1002, 1019	Two structures were built at this locus. Located in the southeast quadrant of the site. (Benn 1992, 478)
1104	1104, 1007	Two, possibly three, structures built here. Located on the western edge of the site. (Benn 1992, 498)

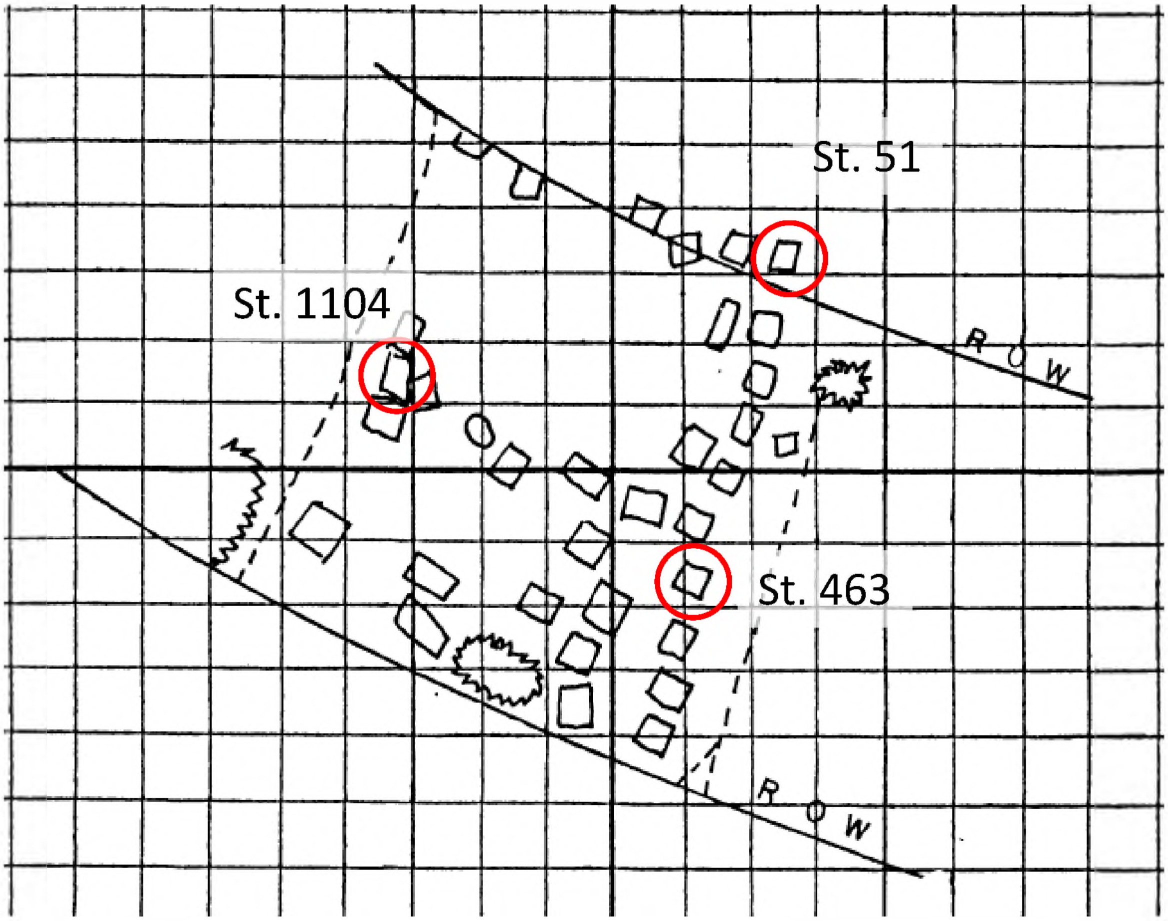

Figure 18. Schematic map of the structures and extent of excavations at the Moon site indicating the structures used in this study. Grid lines are spaced at 10 m intervals and the orientation is north. Map is adapted from Benn (1992, Figure 3.13)

Table 5. Sample of values for five sherds from Structure 51. These values show the count of shell in each size grade after the counts are normalized by column.

Sample	Size 1 Count (Smallest) (Normalized)	Size 2 Count (Medium Small) (Normalized)	Size 3 Count (Medium Large) (Normalized)	Size 4 Count (Largest) (Normalized)
1	0.25	0.06	0.00	0.15
2	0.44	0.55	0.26	0.25
3	0.37	0.14	0.00	0.00
4	0.21	0.17	0.05	0.00
5	0.48	0.34	0.05	0.17

Table 6. Means of the values for the six clusters with notes.

Cluster	Size 1	Size 2	Size 3	Size 4	Count	Notes
1	0.78	0.68	0.42	0.14	11	Lots of small shell
2	0.34	0.53	0.84	0.42	9	Lots of medium-large and large shell
3	0.36	0.44	0.38	0.17	22	Moderate amounts of shell of all sizes
4	0.67	0.75	0.53	0.81	5	Lots of shell temper of all sizes
5	0.21	0.15	0.08	0.05	32	Very few shell
6	0.19	0.21	0.36	0.68	11	Lots of large shell, but not much shell of other size

Table 7. Contingency table showing the count of the number of sherds in each paste mode by household.

Cluster	H. 51	H. 463	H. 1104
1	0	7	4
2	3	1	5
3	10	7	5
4	0	0	5
5	11	12	9
6	6	3	2

Conclusion

In conclusion, this report has shown that it is possible to map, count, and measure shell tempering in exposed sherd edges. The technique for doing so is much more rapid than traditional microscopic petrography and has comparable results. This technique also was able to contribute to our scholarly understanding of inter-sherd variation in temper and inter-household variation in tempering practice.

One limitation of this method of measuring temper in exposed sherd edges is that it requires the temper to have high visual contrast. This holds for shell, but most other ceramic tempers would not be amenable to this procedure. It is possible that with the use of stains or non-visible light specra that a greater range of inclusions of interest to archaeologists and petrographers may be detectable.

As discussed previously, microscopic petrography is not going to diminish in importance any time soon (Livingood and Cordell 2009) because it provides a much more flexible tool for identifying and measuring a far larger range of inclusions. Under the right circumstances, however, digital image analysis of inclusions may be a very effective tool in the prehistorian's and the petrographer's toolit.

Acknowledgements

I want to thank the NCPTT for generously supporting this research. The NCPTT is unique among agencies in supporting technological advancements in preservation and archaeology and as such they perform an invaluable service. As Principal Investigator, I want to thank my consultant, Ann Cordell. She has patiently explained much about petrography through the years and put up with my enthusiasm for new technology. I also want to thank Corson Hirschfeld for spending time teaching me about macro photography and Andrew Fagg for suggesting that a camera might be a more flexible data gathering instrument than a scanner for this project.

References

Benn, David W. 1992. *Excavations at the Moon Site (3Po488), a Middle Mississippian Village in Northeastern Arkansas*. Springfield: Southwest Missouri State University, Center for Archaeological Research, Report No. 780.

———. 1998. "A Fortified Mississippian-Period Village in Poinsett County, Arkansas." In *Changing Perspectives on the Archaeology of the Central Mississippi Valley*, edited by Michael J. O'Brien and Robert Dunnel, 225-257. Tuscaloosa: University of Alabama Press.

Daniels, James, and Carl P. Lipo. 2008. Digital Image Processing of Shell Temper Variability in Late Prehistoric Ceramics. Poster presented at the 73nd Annual Meeting of the Society for American Archaeology. Vancouver, B.C.

Livingood, Patrick C. 2007. "Plaquemine Recipes: Using Computer Assisted Petrographic Analysis to Investigate Plaquemine Ceramic Recipes." In *Plaquemine Archaeology*, edited by Mark A. Rees and Patrick C. Livingood, 108-126. Tuscaloosa: University of Alabama Press.

———. 2010. *Mississippian Polity and Politics on the Gulf Coastal Plain: A View from the Pearl River, Mississippi*. Tuscaloosa: University of Alabama Press.

Livingood, Patrick, and Ann S. Cordell. 2009. "Point/counter point : the accuracy and feasibility of digital image techniques in the analysis of ceramic thin sections." *Journal of Archaeological Science* no. 36 (3):867-872.

Pereira, Carla. 2012. Stylistic Variability within Assemblages of Late Prehistoric Pottery in Lower Mississippi River Valley. Poster presented at the 77th annual meeting of the Society for American Archaeology Meeting. Memphis, TN.

Reedy, Chandra L. 2006. "Review of Digital Image Analysis of Petrographic Thin Sections in Conservation Research." *Journal of the American Institute for Conservation* no. 45 (2):127-146.

Rice, Prudence M. 1987. *Pottery Analysis: A Sourcebook*. Chicago: University of Chicago Press.

Russ, John C. 1999. *The Image Processing Handbook. Third Edition*: CRC Press.

Shepard, Anna O. 1976. *Ceramics for the Archeologist*. Washington, D.C.: Carnegie Institution of Washington.

Stoltman, James B. 1989. "A Quantitative Approach to the Petrographic Analysis of Ceramic Thin Sections." *American Antiquity* no. 54:147-160.

———. 1991. "Ceramic Petrography as a Technique for Documenting Cultural Interaction: An Example from the Upper Mississippi Valley." *American Antiquity* no. 56 (1):103-120.

———. 2000. "The Role of Petrography in the Study of Archaeological Ceramics." In *Earth Sciences and Archaeology*, edited by Vance T. Holliday Paul Goldberg, and C. Reid Ferring, 297-326. Kluwer Academic/Plenum Publishers.

Velde, Bruce, and Isabelle C. Druc. 1998. *Archaeological Ceramic Materials*. Berlin: Springer-Verlag.

Whitbread, I. K. 1991. "Image and data processing in ceramic petrology." In *Recent developments in ceramic petrology*, edited by A. Middleton and I. Freestone, 369-86. London: British Museum Occasional Paper No. 81.